Title	Impact of UV/O_3 treatment on solution-processed amorphous InGaZnO_4 thin-film transistors
Author(s)	Umeda, Kenichi; Miyasako, Takaaki; Sugiyama, Ayumu; Tanaka, Atsushi; Suzuki, Masayuki; Tokumitsu, Eisuke; Shimoda, Tatsuya
Citation	Journal of Applied Physics, 113(18): 184509-1-184509-6
Issue Date	2013-05-13
Type	Journal Article
Text version	publisher
URL	http://hdl.handle.net/10119/11624
Rights	(C) 2013 Author(s). All article content, except where otherwise noted, is licensed under a Creative Commons Attribution 3.0 Unported License. Kenichi Umeda, Takaaki Miyasako, Ayumu Sugiyama, Atsushi Tanaka, Masayuki Suzuki, Eisuke Tokumitsu, and Tatsuya Shimoda, Journal of Applied Physics, 113(18), 184509 (2013) and may be found at http://dx.doi.org/10.1063/1.4804667
Description	

Impact of UV/O3 treatment on solution-processed amorphous InGaZnO4 thin-film transistors

Kenichi Umeda, Takaaki Miyasako, Ayumu Sugiyama, Atsushi Tanaka, Masayuki Suzuki, Eisuke Tokumitsu, and Tatsuya Shimoda
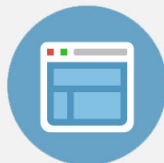
Impact of UV/O₃ treatment on solution-processed amorphous InGaZnO₄ thin-film transistors

Kenichi Umeda,[1,2,a)] Takaaki Miyasako,[1] Ayumu Sugiyama,[1] Atsushi Tanaka,[2] Masayuki Suzuki,[2] Eisuke Tokumitsu,[1,3,4] and Tatsuya Shimoda[1,3,4]

[1]*ERATO, Shimoda Nano-Liquid Process Project, Japan Science and Technology Agency, 2-13 Asahidai, Nomi, Ishikawa 923-1211, Japan*
[2]*FUJIFILM Corporation, Frontier Core-Technology Laboratories, 577 Ushijima Kaisei-Machi, Ashigarakami-Gun, Kanagawa 258-8577, Japan*
[3]*Green Devices Research Center, Japan Advanced Institute of Science and Technology, 2-13 Asahidai, Nomi, Ishikawa 923-1292, Japan*
[4]*School of Material Science, Japan Advanced Institute of Science and Technology, 1-1 Asahidai, Nomi, Ishikawa 923-1292, Japan*

Ultraviolet–ozone (UV/O₃) treatment was adopted to the fabrication of solution-processed amorphous In–Ga–Zn–O thin-film transistors (TFTs), with metal composition of In:Ga:Zn = 1:1:1 represented by InGaZnO₄. By applying UV/O₃ treatment In–Ga–Zn–O gel films, their condensation was notably enhanced through decomposition of organic- and hydrogen-based elements, which drastically improved the quality of the amorphous InGaZnO₄ films. As a result, high TFT performance, with values of on/off ratio, 10^8; subthreshold swing, 150 mV/decade; threshold voltage, 9.2 V; and field-effect mobility, 5.1 cm^2 V^{-1} s^{-1}, was achieved. © *2013 Author(s). All article content, except where otherwise noted, is licensed under a Creative Commons Attribution 3.0 Unported License.* [http://dx.doi.org/10.1063/1.4804667]

I. INTRODUCTION

Amorphous oxide semiconductors such as In–Ga–Zn–O,[1–4] In–Zn–O,[5,6] Zn–Sn–O,[7–10] In–Sn–O,[11] and In–Zn–Sn–O[12,13] have attracted considerable attention as channel materials for next-generation thin-film transistors (TFTs). Compared with crystalline materials, amorphous oxide materials have advantages because of their low processing temperatures and uniformity of device characteristics. In particular, amorphous In–Ga–Zn–O is a promising candidate as an alternative channel material to replace amorphous silicon because high field-effect mobility ($\mu > 1$ cm^2 V^{-1} s^{-1}), steep subthreshold swing (S ≈ 200 mV/decade), low off-current ($I_{off} < 1$ pA), and high stability can be obtained.[14]

Oxide materials containing two or more metal elements are called multicomponent oxide materials. The electrical and material properties of multicomponent oxide materials can be tuned by modulating the metal composition. In the case of sputtered In–Ga–Zn–O materials, optimization of the metal composition has been investigated by the combinatorial approach.[4] It was reported that In had strong influence on mobility, Ga was effective to control the carrier concentration and its tuning attained low off-current in TFTs, and Zn contributed to the modulation of the shallow tail states below the conduction band. An appropriate modulation of the metal composition is important to achieve desirable TFT performance. In sputtered TFTs, the composition region of In–Ga–Zn–O which gives TFTs high performance with normally off operation is approximately In:Ga:Zn = 1:1:1 region represented by InGaZnO₄. In solution-processed TFTs, it has

been investigated that the optimized metal composition region of In–Ga–Zn–O had the same tendency as that of the sputtered counterpart.[15,16]

In the case of solution-processed In–Ga–Zn–O, organic- and hydrogen-based components that remain in the films hinder the forming of the metal–oxide (M-O) bonding network properly. That brings poor performance to resultant TFTs. As many defects are generated, the film quality generally becomes lower than sputtered films. Therefore, a larger amount of In is needed to obtain high mobility ($\mu > 1$ cm^2 V^{-1} s^{-1}).[17–20] Indium oxide can easily generate free carrier because of the oxygen defects so that it is difficult to achieve normally off operation and control the threshold voltage in the In-rich region. If the remaining components in the solution-processed films are reduced, the improved quality of the films would realize high performance TFTs comparable with sputtered InGaZnO₄ ones.

In this study, we focused on the reduction of residual content in gel films to improve the film quality and enhance the M-O bonding network. To reduce the residual content, ultraviolet (UV)/O₃ treatment was introduced. Several papers have reported similar treatments such as UV or plasma for gel films.[21,22] However, they have not been adopted to gel films in the composition region of amorphous InGaZnO₄. We adopted UV/O₃ treatment to the solution-processed In–Ga–Zn–O gel films and obtained high TFT performance composed of amorphous InGaZnO₄.

II. EXPERIMENT

Alkoxide-based In–Ga–Zn–O metal precursor solution was prepared for the fabrication of thin films. At the boiling point of ethanol (78 °C), 0.1 M zinc acetate dihydrate

---

[a)]Author to whom correspondence should be addressed. Electronic mail: kenichi_umeda@fujifilm.co.jp

$(Zn(CH_3COO)_2 \cdot 2(H_2O))$ was synthesized by reflux in ethanol. It was expected that ligands were exchanged from acetate to ethoxide or hydroxide. We added 0.1 M indium isopropoxide $(In–(O–C_3H_7)_3)$ and 0.1 M gallium isopropoxide $(Ga–(O–C_3H_7)_3)$ in diethylaminoethanol (DEAE; $(C_2H_5)_2NC_2H_4OH)$, which stabilizes the solution by chelating, to the zinc solution, and the solution was refluxed at the boiling point of DEAE (163 °C) for 1 h. The mixed solution was condensed by distillation of ethanol and DEAE after stirring for 1 h. The resultant precursor solution had a concentration of 0.1 M In–Ga–Zn–O. The solution was filtered through a 0.2-μm syringe filter (polytetrafluoroethylene) and then spin-coated on the substrate after O_2 plasma cleaning (SAMCO FA-1). Quartz substrates (T-4040) were used for material evaluation.

UV/O_3 treatment was performed to the spin-coated In–Ga–Zn–O gel films by using MHU-110WB (Multiply), as shown in Figure 1. A low-pressure mercury lamp was used as the light source having wavelengths of 185 nm and 254 nm. The light energies at wavelengths of 185 nm and 254 nm were 647 kJ/mol and 472 kJ/mol, respectively. These values are larger than the bonding energy of the organic- and hydrogen-based content such as C–H (413 kJ/mol), C–C (348 kJ/mol), and C–O (352 kJ/mol). Both the UV lights, 185 nm and 254 nm, have the ability to decompose these residual contents. Furthermore, O_3 is generated by irradiation at 185 nm because of decomposition to ground state of O atom from O_2 molecules and combination of O atom and O_2 molecules $(O_2 + h\nu \ (185 \ nm) \rightarrow O + O)$, and radical oxygen (O^*) is generated at 254 nm because of decomposition to O^* and O_2 molecules from O_3 $(O_3 + h\nu \ (254 \ nm) \rightarrow O^* + O_2)$.
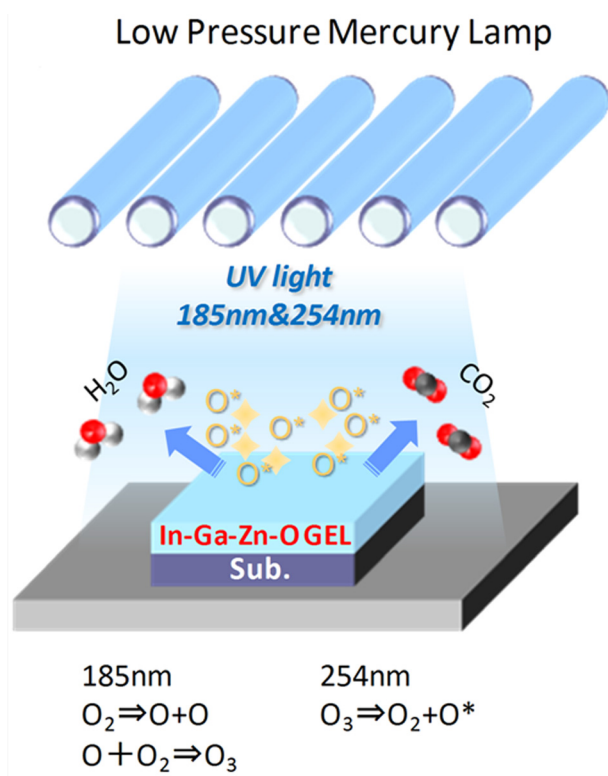
These elements assist the removal of organic- and hydrogen-based compounds after decomposition. Therefore, this process was expected to enhance formation of the M-O bonding network and lower the process temperature.

To clarify the roles of UV and O_3, UV-1 (SAMCO) which equips with an atmosphere control system and an ozonizer was used. The effect of UV light was evaluated by its irradiation in N_2. The effect of O_3 was evaluated by the ozonizer, which generates O_3 without UV irradiation. To clarify the effect of the combination of UV and O_3, UV light was irradiated in O_2 atmosphere. This condition increases the concentration of O_3 generated by UV irradiation under O_2 atmosphere. After UV/O_3 treatment, an annealing process was conducted in O_2 (20%) and N_2 (80%) atmosphere.

To observe the thermal decomposition behavior, thermogravimetric and differential thermal analysis (TG-DTA, Seiko Instruments Inc.) were performed under O_2 (20%) and N_2 (80%) atmosphere at a heating rate of 10 °C min^{-1}. An amorphous or a crystal phase was determined by X-ray diffraction (XRD, Rigaku Ultima III diffractometer with Cu Kα radiation) using a fixed glancing incidence angle (0.4°) (GI-XRD). The metal composition of films was evaluated by X-ray fluorescence analysis (XRF, Panalytical Axios). Fourier transform infrared spectrophotometry (FT-IR, Bruker Alpha-T) was performed to investigate the organic bonding states (such as C–H and C–O) of films by attenuated total reflectance geometry. The condensation of the oxide gel films was evaluated by thermal desorption spectroscopy (TDS). The metal oxide bonding state was investigated by X-ray photoelectron spectroscopy (XPS, Kratos AXIS-ULTRA DLD).

Bottom-gate and top-contact TFTs were fabricated using solution-processed amorphous InGanZnO$_4$ films as a channel layer. The structure of the fabricated TFTs is shown at Figure 2. Heavily boron (p$^+$) doped silicon (<0.02 Ω cm) wafers were used as gate electrodes, and silicon dioxide (100 nm) formed by thermal oxidation was used as a gate insulator. The solution-processed amorphous InGaZnO$_4$ films (20 nm) with and without UV/O_3 treatment were adopted as a channel layer. Molybdenum with the thickness of 100 nm was used for source and drain electrodes. The channel length and width were 20 and 60 μm, respectively. The TFT characteristics were measured using a semiconductor parameter analyzer (Agilent HP 4145) at room temperature in a dark room.

III. RESULTS AND DISCUSSION

Figure 3(a) shows the TG-DTA results for the In–Ga–Zn–O solution. It was confirmed that the pyrolysis
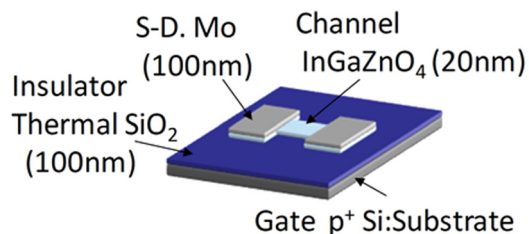

FIG. 1. UV/O_3 treatment schematic.

FIG. 2. Structure of the solution-processed amorphous InGaZnO$_4$ TFT on Si/thermal SiO$_2$ substrate.
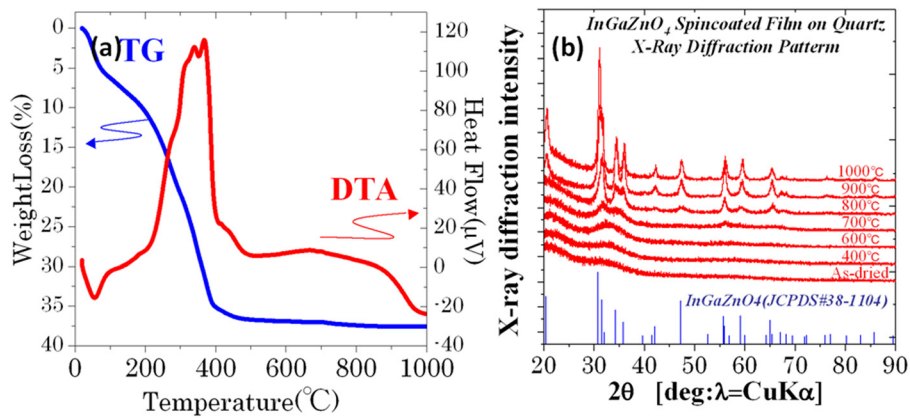
FIG. 3. (a) TG-DTA characteristics of In–Ga–Zn–O precursor solution and (b) the annealing temperature dependence of the glazing incident X-ray diffraction pattern of the solution-processed InGaZnO4 film (100 nm).

temperature was approximately 400 °C, and In–Ga–Zn–O gel was converted to an InGaZnO4 metal oxide solid. Figure 3(b) shows dependence of the XRD patterns on the annealing temperature of the InGaZnO4 films without UV/O3 treatment. The InGaZnO4 films with annealing temperatures below 600 °C were in an amorphous state. These results clarified that an amorphous metal oxide film could be obtained with an annealing temperature between 400 and 600 °C. The crystalline temperature was over 700 °C, and single-phase InGaZnO4 (JCPDS No. 38-1104) appeared at a temperature of more than 800 °C. A previous study reported the same tendency as this for a sputtered film.[3] The metal composition of the InGaZnO4 film after annealing at 600 °C was In:Ga:Zn = 1:0.98:0.95. In this metal composition region, it is difficult to obtain high mobility ($\mu > 1$ cm^2 V^{-1} s^{-1}) as explained in Sec. I. It is considered that these results show an adverse implication of the residual carbon- and hydrogen-based content.

To decompose and remove these contents effectively, UV/O3 treatment was conducted in air atmosphere. Figure 4(a) shows the FT-IR spectral change of the In–Ga–Zn–O gel films by UV/O3 treatment. The broad peak around the region from 2500 cm^{-1} to 3700 cm^{-1} show the presence of OH stretching vibrations (Figure 4(b)). This peak shifted to a low wavenumber after UV/O3 treatment for 30 min. In the region of OH stretching vibration, the high wavenumber region was because of the free state of metal–hydroxide (M-OH) bonding without hydrogen bonding, and the low

wavenumber region was because of the state of the M-OH network with hydrogen bonding.[23] It is considered that the free state of M-OH bonding was decomposed by the UV/O3 treatment.

The sharp peaks at approximately 3000 cm^{-1} were eliminated by the treatment for 5 min. These peaks were related to the stretching vibrations of CH2 and CH3 groups of unhydrolyzed alkoxides. These C–H based contents were decomposed and removed by the treatment for a short time.

The band at approximately 1500 cm^{-1} in Figure 4(a) shows a curious spectral change. It is considered that the change was related to C–O- and C–C-based contents. The sharp peaks at 1570 and 1415 cm^{-1} without UV/O3 treatment show symmetric and asymmetric vibrations of C=O bonding. This bonding suppresses the condensation of the oxide gel films by chelating with coordination bonding to the metal elements.[24] It is expected that the condensation was promoted by decomposing this bonding. After 30 min of UV/O3 treatment, this bonding was decomposed, and two new symmetrical peaks are observed at 1500 cm^{-1} and 1395 cm^{-1}, center fitted by Gaussian peaks in Figure 4(c). As a hypothesis, it is considered that these peaks are related to amorphous carbon because they are similar to the Raman-active G (graphite-like carbon) and D (disordered carbon) bands.[25–27] Therefore, ligands could be decomposed by the UV/O3 treatment and transformed to the state like amorphous carbon. In order to clarify the origin of these peaks, further investigations are required.
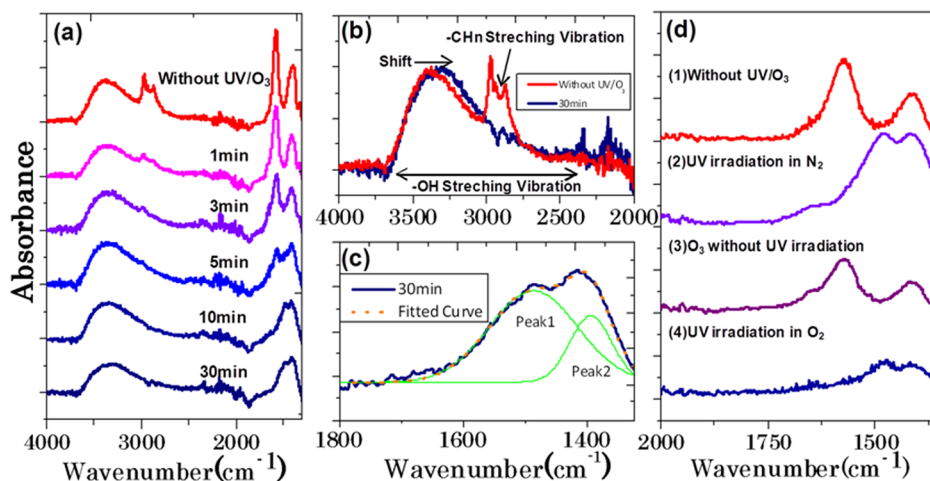

FIG. 4. (a) Time dependence of UV/O3 treatment at air atmosphere on FT-IR spectra of In–Ga–Zn–O gel film (50 nm). (b) Extracted normalized figure in the 2000–4000 cm^{-1} region of UV/O3 treatment for 0 and 30 min. (c) Extracted and Gaussian fitting results in the 1300–1800 cm^{-1} region after UV/O3 treatment for 30 min. (d) Parameter comparison of UV/O3 treatment for In–Ga–Zn–O gel film.
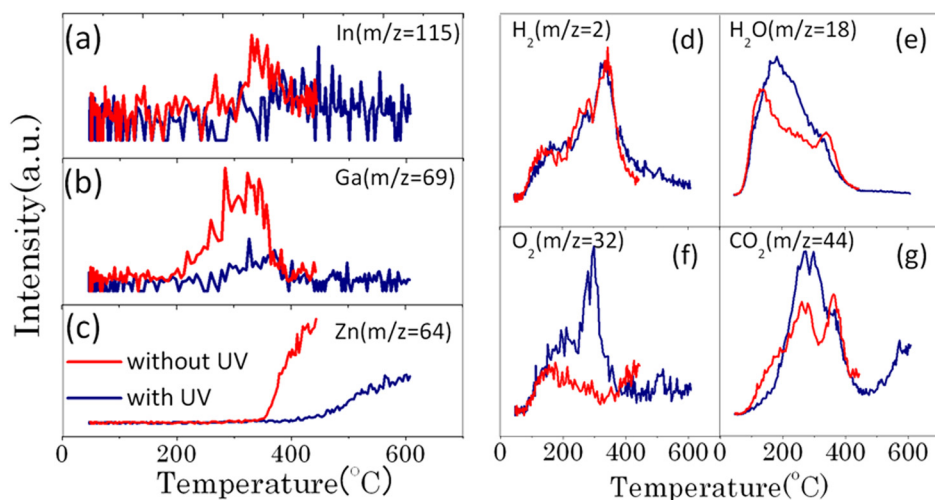
FIG. 5. TDS spectra of In–Ga–Zn–O gel film (50 nm) with and without UV/O_3 treatment. (a)–(c) Metal content (In, Ga, Zn) and (d)–(g) carbon, hydrogen, and oxygen content (H_2, H_2O, O_2, CO_2).

In addition, atmosphere dependence was investigated to clarify the roles of UV and O_3. The FT-IR spectra shape was changed by UV irradiation in N_2 (Figure 4(d-2)). In the case of O_3 irradiation without UV, the spectra shape was not changed and the peak intensity was slightly reduced (Figure 4(d-3)). It was clarified that UV light was the parameter for the decomposition of the ligands such as C=O and C–H bonding, and O_3 was the parameter for the removal of the decomposed contents. To investigate the combination of UV and O_3, UV light was irradiated in O_2 atmosphere. Figure 4(d-4) shows the change and reduction of the FT-IR spectra at approximately 1500 cm^{-1}. In summary, it is reasonable to conclude that both UV and O_3 irradiation are necessary to reduce the residual contents in the gel films effectively.

TDS measurement was conducted to evaluate the condensation in In–Ga–Zn–O gel films with and without UV/O_3 treatment. To remove the influence of self-heating during the treatment, 120 °C process was performed for the sample with and without UV/O_3 treatment. The treatment was performed for 30 min at air atmosphere. Figures 5(a)–5(c) show the

desorption behavior of the metal contents. The amount of desorption of Zn was greater than those of In and Ga. Zn tends to form unstable chemical bonds.[28] The total amount of desorption of metal content was decreased by the UV/O_3 treatment. The condensation in InGaZnO$_4$ gel films was clearly promoted by the UV/O_3 treatment. Figures 5(d)–5(g) show the amount of desorption of organic- and hydrogen-based content. The desorption of O_2, H_2O, and CO_2 was greater for InGaZnO$_4$ gel films with UV/O_3 treatment than without it. It is considered that with UV/O_3 treatment, the organic- and hydrogen-based content was easily desorbed by the decomposition of the ligand state.

The characteristics of the annealed InGaZnO$_4$ films were investigated by comparing the results from the treatment with and without UV/O_3. The UV/O_3 treatment at air atmosphere was performed for 30 min. To confirm the amorphous state of the annealed InGaZnO$_4$ films with UV/O_3 treatment, the annealing temperature dependence of GI-XRD was measured (Figure 6). The InGaZnO$_4$ films with UV/O_3 treatment showed an amorphous state after annealing at 600 °C. The same result was shown in the InGaZnO$_4$ films without UV/O_3 treatment. Figure 7 shows dependence of the binding energy of the O$_{1s}$ measured by XPS on the annealing temperature. The peak intensity of M-OH bonding decreased
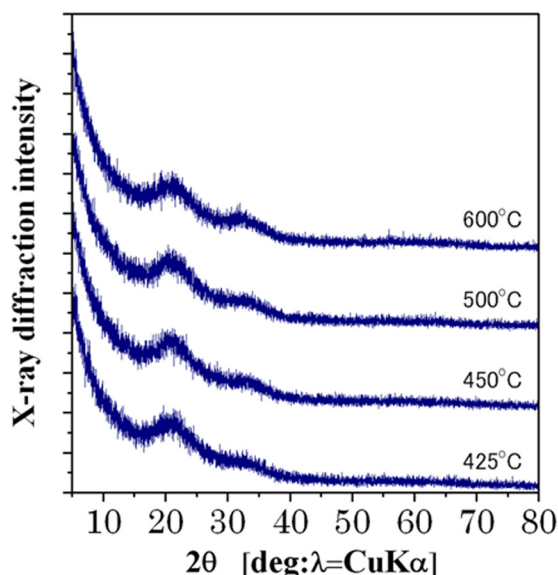

FIG. 6. Annealing temperature dependence of GI-XRD with UV/O_3 treatment.
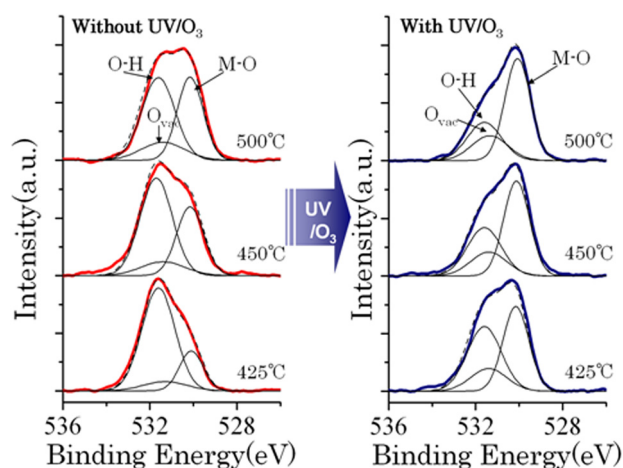

FIG. 7. Annealing temperature dependence of XPS for the O$_{1s}$ region of alkoxide-based InGaZnO$_4$ with and without UV/O_3 treatment.
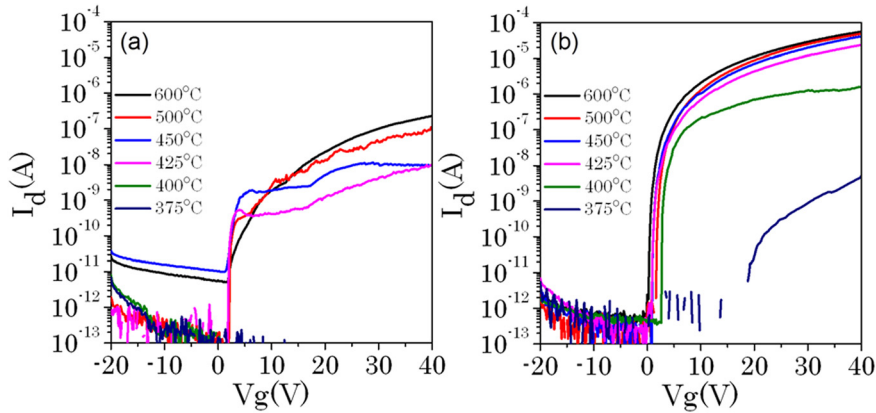
FIG. 8. Annealing temperature dependence of the TFT transfer characteristics of InGaZnO$_4$ TFT on Si/thermal SiO$_2$ substrates with and without UV/O$_3$ treatment ($V_{ds} = 5$ V, L/W = 20 μm/60 μm); (a) without UV/O$_3$ treatment and (b) with UV/O$_3$ treatment.

and the peak intensity of M-O bonding clearly increased with the UV/O$_3$ treatment. The formation of a M-O bonding network is closely related to device properties, and it is expected that the TFT characteristics can be improved by UV/O$_3$ treatment of gel films.

Figure 8 shows the annealing temperature dependence of the transfer characteristics of I$_D$ versus V$_G$ at V$_{DS}$ = 5 V (Figure 8(a), without UV/O$_3$ treatment; Figure 8(b), with UV/O$_3$ treatment). The transfer characteristics were improved with UV/O$_3$ treatment. The field-effect mobilities (μ_{lin}) of the TFTs were calculated using the following equation: I$_{DS}$ = (W/L) μ_{lin} CV$_{DS}$ (V$_G$ − V$_{TH}$), where I$_{DS}$ is the drain current, V$_{TH}$ is the threshold voltage, W and L are the channel width and length, respectively, and C is the capacitance per unit area of the gate dielectric.

For the solution-processed amorphous InGaZnO$_4$ TFT with UV/O$_3$ treatment, the following results were obtained after annealed at 500 °C: on/off ratio, 10^8; subthreshold swing, 150 mV/decade; field-effect mobility, 5.1 cm^2 V^{-1} s^{-1}; and threshold voltage, 9.2 V. These results show the typical enhancement-type operation of the normally off property. Each parameter is comparable to the parameters of a sputter-processed amorphous InGaZnO$_4$ TFT. The plot of mobility versus annealing temperature is shown in Figure 9. By using UV/O$_3$ treatment, high mobility (>1 cm^2 V^{-1} s^{-1}) was

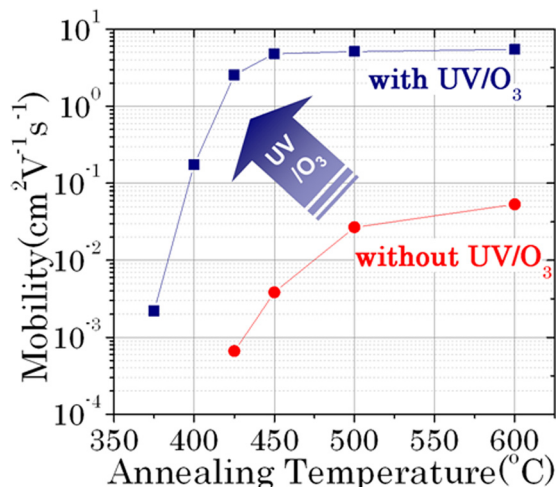achieved at a lower process temperature (425 °C). The TFT performance was drastically improved and process temperature became lower with UV/O$_3$ treatment.

IV. SUMMARY

We synthesized the alkoxide-based metal precursor solution of InGaZnO$_4$ for the channel layers of TFTs. To improve the quality of this film, UV/O$_3$ treatment was introduced. This treatment is effective to decompose organic- and hydrogen-based contents and enhance the condensation in In–Ga–Zn–O gel films. In addition, it was observed that formation of the M-O bonds of an amorphous InGaZnO$_4$ film was drastically accelerated with UV/O$_3$ treatment. By using this process, the TFT performance was improved and process temperature became lower. The obtained field-effect mobility, on/off ratio, threshold voltage, and subthreshold swing were 5.1 cm^2 V^{-1} s^{-1}, 10^8, 9.2 V, and 150 mV/decade, respectively. These values are applicable to high-performance display backplanes. In addition, a high mobility (>1 cm^2 V^{-1} s^{-1}) was achieved at a lower process temperature (425 °C). This metallic composition of InGaZnO$_4$ is almost the same as that of the sputtered counterpart and shows high TFT performance because of the improved quality of the solution-processed amorphous InGaZnO$_4$ films with UV/O$_3$ treatment. Therefore, we believe that this solution-based process and UV/O$_3$ treatment are promising candidates for use in printed electronics applications.

FIG. 9. Annealing temperature dependence of mobility with and without UV/O$_3$ treatment.

[1]K. Nomura, H. Ohta, A. Takagi, T. Kamiya, M. Hirano, and H. Hosono, Nature **432**, 488 (2004).
[2]H. Yabuta, M. Sano, K. Abe, T. Aiba, T. Den, H. Kumomi, K. Nomura, T. Kamiya, and H. Hosono, Appl. Phys. Lett. **89**, 112123 (2006).
[3]K. Nomura, A. Takagi, T. Kamiya, H. Ohta, M. Hirano, and H. Hosono, Jpn. J. Appl. Phys., Part 1 **45**, 4303 (2006).
[4]T. Iwasaki, N. Itagaki, T. Den, H. Kumomi, K. Nomura, T. Kamiya, and H. Hosono, Appl. Phys. Lett. **90**, 242114 (2007).
[5]B. Yaglioglu, H. Y. Yeon, R. Beresford, and D. C. Paine, Appl. Phys. Lett. **89**, 062103 (2006).
[6]P. Arquinha, A. Pimente, A. Marques, L. Pereira, R. Martins, and E. Fortunato, J. Non-Cryst. Solids **352**, 1749 (2006).

[7]H. Q. Chiang, J. F. Wager, R. L. Hoffman, J. Jeong, and D. A. Keszler, Appl. Phys. Lett. **86**, 013503 (2005).

[8]W. B. Jackson, R. L. Hoffman, and G. S. Herman, Appl. Phys. Lett. **87**, 193503 (2005).

[9]P. Gorrn, M. Sander, J. Meyer, M. Kroger, E. Becker, H.-H. Johannes, W. Kowalsky, and T. Riedl, Adv. Mater. **18**, 738 (2006).

[10]R. L. Hoffman, Solid-State Electron. **50**, 784 (2006).

[11]T. Miyasako, M. Senoo, and E. Tokumitsu, Appl. Phys. Lett. **86**, 162902 (2005).

[12]M. S. Grover, P. A. Hersh, H. Q. Chiang, E. S. Kettenring, J. F. Wager, and D. A. Keszler, J. Phys. D **40**, 1335 (2007).

[13]K. J. Saji, M. K. Jayaraj, K. Namura, T. Kamiya, and H. Hosono, J. Electrochem. Soc. **155**, H390 (2008).

[14]T. Kamiya, K. Nomura, and H. Hosono, Sci. Technol. Adv. Mater. **11**, 044305 (2010).

[15]D. Kim, C. Y. Koo, K. Song, Y. Jeong, and J. Moon, Appl. Phys. Lett. **95**, 103501 (2009).

[16]Y. H. Kim, M. K. Han, J. I. Han, and S. K. Park, IEEE Trans. Electron Devices **57**, 1009 (2010).

[17]S. Jeong, Y.-G. Ha, J. Moon, A. Facchetti, and T. J. Marks, Adv. Mater. **22**, 1346 (2010).

[18]D. Kim, Y. Jeong, C. Y. Koo, K. Song, and J. Moon, Jpn. J. Appl. Phys., Part 1 **49**, 05EB06 (2010).

[19]G. H. Kim, W. H. Jeong, and H. J. Ki, Phys. Status Solidi A **207**(7), 1677 (2010).

[20]Y. Wang, S. W. Liu, X. W. Sun, J. L. Zhao, G. K. L. Goh, Q. V. Vu, and H. Y. Yu, J. Sol-Gel Sci. Technol. **55**, 322 (2010).

[21]Y.-H. Kim, J.-S. Heo, T.-H. Kim, S. Park, M.-H. Yoon, J. Kim, M. S. Oh, G.-R Yi, Y.-Y. Noh, and S. K. Park, Nature **489**, 128 (2012).

[22]P. K. Nayak, M. N. Hedhili, D. Cha, and H. N. Alshareef, Appl. Phys. Lett. **100**, 202106 (2012).

[23]M. L. Hair, J. Non-Cryst. Solids **19**, 299 (1975).

[24]M. Ivanda, S. Music, S. Popovic, and M. Gotic, J. Mol. Struct. **480**, 645 (1999).

[25]N. Nakayama, Y. Tsuchiya, S. Tamada, K. Kosuge, S. Nagata, K. Takahiro, and S. Yamaguch, Jpn. J. Appl. Phys., Part 2 **32**, L1465 (1993).

[26]R. O. Dillon, J. A. Woollam, and V. Katkanant, Phys. Rev. B **29**, 3482 (1984).

[27]A. C. Ferrari and J. Robertson, Phys. Rev. B **61**, 14095 (2000).

[28]K. Nomura, T. Kamiya, H. Ohta, M. Hirano, and H. Hosono, Appl. Phys. Lett. **93**, 192107 (2008).